

## Automatic detection of bulldozer-induced changes on a sandy beach from video using YOLO algorithm

Barbero-García, Inés; Kuschnerus, Mieke; Vos, Sander; Lindenbergh, Roderik

**DOI**

[10.1016/j.jag.2023.103185](https://doi.org/10.1016/j.jag.2023.103185)

**Publication date**

2023

**Document Version**

Final published version

**Published in**

International Journal of Applied Earth Observation and Geoinformation

**Citation (APA)**

Barbero-García, I., Kuschnerus, M., Vos, S., & Lindenbergh, R. (2023). Automatic detection of bulldozer-induced changes on a sandy beach from video using YOLO algorithm. *International Journal of Applied Earth Observation and Geoinformation*, 117, Article 103185. <https://doi.org/10.1016/j.jag.2023.103185>

**Important note**

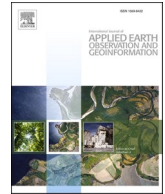
To cite this publication, please use the final published version (if applicable). Please check the document version above.

**Copyright**

Other than for strictly personal use, it is not permitted to download, forward or distribute the text or part of it, without the consent of the author(s) and/or copyright holder(s), unless the work is under an open content license such as Creative Commons.

**Takedown policy**

Please contact us and provide details if you believe this document breaches copyrights. We will remove access to the work immediately and investigate your claim.



# Automatic detection of bulldozer-induced changes on a sandy beach from video using YOLO algorithm

Inés Barbero-García<sup>a,\*</sup>, Mieke Kuschnerus<sup>b</sup>, Sander Vos<sup>c</sup>, Roderik Lindenbergh<sup>b</sup>

<sup>a</sup> Department of Cartography and Terrain Engineering, Polytechnic School of Ávila, University of Salamanca, Hornos Caleros 50, 05003 Ávila, Spain

<sup>b</sup> Department of Geoscience and Remote Sensing, Delft University of Technology, Delft, The Netherlands

<sup>c</sup> Department of Hydraulic Engineering, Delft University of Technology, Delft, The Netherlands

## ARTICLE INFO

### Keywords:

Coastal monitoring  
Object detection  
Principal components analysis  
Anthropogenic changes

## ABSTRACT

Sandy beaches are subject to changes due to multiple factors, that are both natural (e.g. storms) and anthropogenic. Great efforts are being made to monitor these ecosystems and understand their dynamics in order to assure their conservation. The identification of anthropogenic changes and its differentiation from natural ones is an important task for coastal monitoring. In this study, we present a methodology for the detection of anthropogenic changes in a coastal ecosystem by automatically detecting active bulldozers in continuous beach video data. PCA is used to highlight changes in consecutive images due to moving objects. Next, the YOLO object detection algorithm is used to identify the bulldozers in the change images. YOLO was specifically trained for the task, obtaining a precision of 0.94 and a recall of 0.81. An automatic tool was developed, and the process was carried out on two months of video data, consisting of approximately 19 000 images. The resulting information was compared with changes derived from 3D data obtained from a permanent laser scanner. The correlation among the results of the two methodologies was computed. For a validation area and daily time frame a correlation of 0.88 was obtained between the number of detected bulldozers and the area affected by changes in height larger than 0.3 m.

## 1. Introduction

Coastal dunes and sandy beaches are ecosystems subject to constant change due to erosion and accretion of sand. Climate change and rise of sea level, in combination with human intervention, are factors that greatly impact these ecosystems (Paprotny et al., 2021; Stronkhorst et al., 2018). The accurate and continuous monitoring of these areas is required as it is vital for the development of sustainable strategies for their conservation.

Coastal erosion and accretion are greatly affected by factors such as sea level rise, increase in frequency and strength of storms, land subsidence or changes in river sediment, mostly as a consequence of dam construction (Mentaschi et al., 2018; Stronkhorst et al., 2018). Beach areas are also affected by anthropogenic processes that involve direct movement of sand. These direct anthropogenic changes include beach nourishments, grooming, recreational use or the use of off-road vehicles (Defeo et al., 2009). Beach nourishing has become a common practice in many locations (De Schipper et al., 2021). During this process, large quantities of sand are added to the beach to elevate it and increase its

size (Peterson and Bishop, 2005), and the process must be repeated periodically as it does not prevent from future erosion (Landry, 2011). Beach grooming is common in recreational areas and involves important sand movements that greatly affect the natural environment (Barros, 2001; Davenport and Davenport, 2006; Costa et al., 2022).

Beach ecosystems have high socioeconomic value. Therefore, coastline retreat has important economic impact on property owners, recreational users and local businesses (Landry, 2011; Paprotny et al., 2021). Additionally, the protective function of the coastal area as a defense against floods and storm surges needs to be maintained. The preservation of the coast and connected ecosystems is in line with the Sustainable Development Goals (United Nations, 2015), in particular the section on Climate Action (Kandrot et al., 2022).

Around one third of world coastlines are sandy beaches, which are also specifically affected by human activities, both direct (Defeo et al., 2009; Peterson and Bishop, 2005) and indirect (Luijendijk et al., 2018; Vos et al., 2022). Human intervention can be a starting point of erosive processes, generating areas of high vulnerability (de Andrade et al., 2019; List et al., 2006). In the Netherlands, human interventions on

\* Corresponding author.

E-mail address: [ines.barbero@usal.es](mailto:ines.barbero@usal.es) (I. Barbero-García).

sandy beaches are regulated by the Ministry of Infrastructure and Water Management (Rijkswaterstaat). Displacement of sand is allowed up to a specified threshold. The regulation is difficult to enforce on a regular basis and consequences of the chosen threshold value are not studied. Close-range monitoring of an exemplary section of the coast and all anthropogenic activities affecting the sand volume and distribution, serves as a case study to analyze the individual and compound impact of many small-scale interventions, that went unnoticed in the past. Such impact assessment is expected to give insight in the usability of the current regulations. The present study relies on data obtained as part of the CoastScan project (Vos et al., 2017). The objective of this project was to develop a monitoring system to understand coastal dynamics during long time periods by the acquisition of detailed topographic data. A permanent laser scanner was used to obtain hourly 3D data at Noordwijk, (Netherlands), for several years. For a smaller period, corresponding to approximately 2 months, in 2020, videos of the scanned area were also acquired. The objective of these videos was to evaluate the possibilities of the image information to complement and improve the understanding of the acquired 3D data. The characteristics of the chosen location as a typical urban beach on the Dutch coast, makes it representative for urban, dissipative beaches (Ruessink and Jeuken, 2002).

The use of video has become a common low-cost technology for coastal monitoring (Quartel et al., 2006; Nieto et al., 2010), being the objective of important projects such as ARGUS (Holman and Stanley, 2007) or COSMOS (Taborda and Silva, 2012). Other video data sources, not specifically designed for coastal monitoring, such as the surfcams, have proven great usability in coastal monitoring (Andriolo et al., 2019; Conlin et al., 2020).

The large amount of data generated by continuous monitoring of the environment presents a challenge for the adequate processing (Anders et al., 2021). Automatic processing techniques are required to extract useful information from such data.

Previous works on the CoastScan project focused on the identification and extraction of surface changes from 3D data (Anders et al., 2021; Kuschnerus et al., 2021). In order to properly understand the results, it is required to distinguish between anthropogenic and natural changes. However, no ground truth is available to make this distinction. The reliable and automatic identification of anthropogenic changes is, therefore, a limitation to be solved (Kuschnerus et al., 2021; Kuschnerus et al., 2022).

The image data was considered a useful tool for identification of these human interventions. In particular, the bulldozers working on the sand are easily identified. Bulldozer works represent an important percentage of human impact on sandy coastlines (Lazarus and Goldstein, 2019). In particular they are used for beach nourishment (Lazarus et al., 2011), creation of artificial dunes or defenses against storm events (Magliocca et al., 2011), cleaning, and maintenance of access paths. Dutch regulation allows a limited volume of sand to be moved by individuals with a relevant license (as owners of beach clubs), however, the rule is difficult to enforce (Kuschnerus et al., 2022). In the particular location of study, bulldozers are commonly used to create embankments before storms and to remove sand from areas of deposition after storm events, the levelling of some areas to create recreational areas with tables and loungers is also common.

Machine Learning algorithms are becoming a common approach for environmental monitoring. In particular, YOLO (You Only Look Once) (Redmon et al., 2016) is an object detection algorithm that uses conventional neural networks and has provided outstanding results in object detection for a wide range of applications. Its high speed allows for accurate object detection in real time. Its environmental applications include the detection of litter (Lin et al., 2021; Veerasingam et al., 2022), forest snow damage (Puliti and Astrup, 2022), forest fires (Xu et al., 2021) or different fish species (Jalal et al., 2020).

In this paper, we apply the YOLO algorithm to detect bulldozers on coastal video data. Firstly, the video frames were extracted and

preprocessed using Principal Components Analysis (PCA) (Abdi and Williams, 2010), a well-known methodology to highlight moving or changing objects in images (Deng et al., 2008; Ingebritsen and Lyon, 1985; Lu et al., 2005). YOLOv5 was specifically trained for the detection of the bulldozers on this type of images. Later, the detection was carried out for the two months of the CoastScan image dataset and the detected sand movements as carried out by bulldozers were validated in comparison with suspected anthropogenic changes detected from the 3D data.

The novelty of the presented study relies in three main points:

Change images, obtained using PCA are used as the input for YOLO detection. Although PCA has been used to reduce dimensionality prior to YOLO detection (Masoom et al., 2022), to the knowledge of the authors there are no previous studies that combine PCA change detection and YOLO to identify changing objects in video images.

The validation of the results was carried out by reprojecting the detected bulldozers position to the coordinate system of the scanner and comparing the results with the changes obtained from detailed 3D data.

The procedure was carried out automatically for a large dataset of approximately 19 000 images.

## 2. Materials and methods

This section is divided in (i) description of the study area, (ii) the description of the CoastScan data, (iii) description of the YOLO algorithm, (iv) methodology for bulldozer detection, including YOLO training and detection of bulldozers for the whole CoastScan image dataset, and (v) matching of the obtained results with notably laser-derived 3D changes.

### 2.1. Study area

The area of study is the beach of Noordwijk, in the Netherlands (Fig. 1). The covered area is approximately 950 m long and 250 m wide. It includes the sandy beach, the dune area, a paved area, path and stairs leading to the beach and a beach club building located on the boundary between dunes and beach.

### 2.2. Study area data

The CoastScan dataset is composed of laser-derived 3D data and video data.

For the 3D data a Riegl VZ-2000 laser scanner was placed on the top floor of a hotel building, located behind the dunes and at 55 m above sea level. A scan of the whole area is acquired every hour.

Two cameras were positioned next to as the scanner between February 20 and April 26, 2020. For the period between February 29 and April 24 the dataset can be considered constant, with some small gaps that should not affect the results. For the period between the February 20 and February 28, the videos are fragmented and cover only some periods of the day with no data registered for the 27th. For the last day, April 26, the video stops in the morning as the camera is removed from its location.

The time interval between image acquisition is not constant and varies from 5 Hz to 6.6 mHz (five images per second to one image every 2.5 min). Camera 1 is pointing directly to the ocean and covers the whole study area (Fig. 2a). Camera 2 is pointing diagonally and covers only a part of the study area (Fig. 2b). The resolution of the images is 1912x1088 pixels.

The dataset provides a useful source of data with high quality images and image frequency. Nevertheless, some of the particularities of the images hamper the detection of bulldozers, people or other agents interacting with the beach. In the first place, the images cover a large area, and therefore the bulldozers have a small size in pixels (i.e. between 20 and 70 pixels in most cases). Moreover, the quality of the images varies due to the weather conditions, so blurred images can be



Fig. 1. Location of study area in Noordwijk, the Netherlands. Image from ESRI World Imagery.



Fig. 2. CoastScan project video frames for camera 1 (a) and camera 2 (b).

expected for rainy days. An example of the images can be seen in Fig. 2.

Night images are also taken and needed to be automatically removed during the preprocessing stage.

The weather data for the location was obtained by the Royal Netherlands Meteorological Institute (KNMI). In particular the wind speed and direction is available for every hour.

### 2.3. The YOLO algorithm

YOLO is a state-of-the-art object detection algorithm that uses a single convolutional network. Six generations of YOLO have been released. In this study we apply YOLOv5, which presents important improvements in terms of accuracy and speed in comparison with previous versions. YOLO consist of (i) Backbone (CPSDarknet) for feature extraction, (ii) Neck (Panet) for feature fusion and (iii) Head (YOLO layer) for generating the detection results.

The YOLO algorithm divides the image into grids, bounding boxes and the confidence of them containing an object are predicted for each grid. Ideally, the confidence score should be zero if there is no object in that cell and equal to the intersection over union between the ground truth and the predicted box if an object exists.

Separately, a set of class probabilities is predicted for each grid.

In the last stage, the class probability of each bounding box is multiplied by the confidence score producing a class-specific confidence score. These scores reflect the probability of a class appearing in the box and how well the box fits the object. The class with the highest class-specific confidence score is selected as the final prediction (Redmon et al., 2016).

YOLOv5 provides 5 different models with different network depth and feature map width. The model used in this study is YOLOv5s, as it

was found to provide the best results after several tests.

### 2.4. Bulldozer detection

The use of YOLO for bulldozer detection requires training the algorithm. The model training process consists of (i) frame extraction, (ii) generation of change images, (iii) image cropping, (iv) labelling, (v) model training and (vi) model evaluation. The detection of bulldozers is carried out for the whole set of videos, as acquired by CoastScan Camera 1. The bulldozer detection process consists of (i) frame extraction, (ii) image correction, (iii) generation of change images, (iv) image cropping, (v) bulldozer detection using YOLO, (vi) coordinate extraction and (vii) filtering (Fig. 4).

#### 2.4.1. Model training

**2.4.1.1. Training data.** The available CoastScan dataset contains an important number of images, however, it is limited in terms of variability, as all the images belong to the same location with two different points of view. In order to enrich the dataset with a larger quantity of images and locations, two more data sources were included for training. The second set of images was obtained from the ARGUS project (Holman and Stanley, 2007), in a location named Zandmotor, south of The Hague, The Netherlands (Fig. 3a). The third set of images was obtained from the Coastal Ocean Observatory (COO) for the location of Castelldefels, Spain, these data are available at ICM-CSIC (<https://coo.icm.csic.es/>) (Fig. 3b).

The CoastScan dataset is composed of videos covering a period between 34 min and one day, the minimum frequency is one image every 2.5 min.



Fig. 3. Images with visible bulldozers (highlighted in red) from ARGUS dataset (a) and COO dataset (b). (For interpretation of the references to colour in this figure legend, the reader is referred to the web version of this article.)

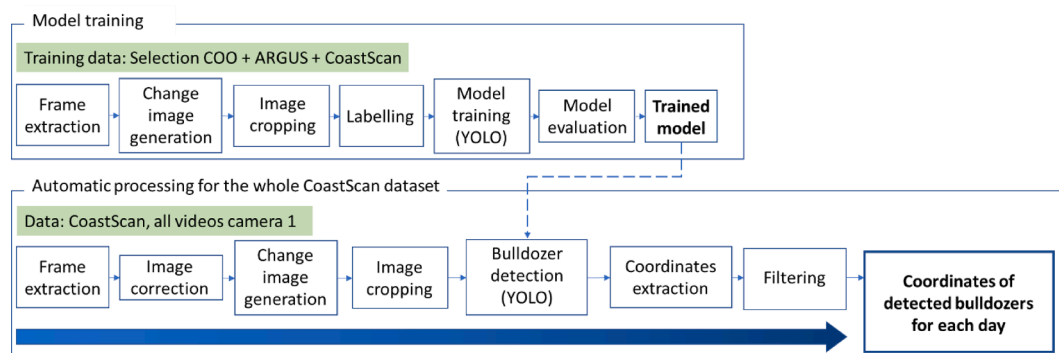


Fig. 4. Workflow of the training of the YOLO algorithm and the consecutive detection.

For the ARGUS data, one image is available every 30 min, while the COO dataset consists of one image every hour.

**2.4.1.2. Frame extraction.** Firstly, videos or images of days with working bulldozers were manually identified. It was not possible to analyse every image of each dataset due to the large quantity of data. Instead, the periods after storms were found and checked for bulldozers.

For the CoastScan dataset, frames were extracted for each selected video. Frames corresponding to night hours or otherwise too dark were removed by using a mean value threshold. As videos present different frequencies, the whole dataset was resampled to 6.6 mHz (approximately 1 image every 2.5) minutes. The image frequency is considered sufficiently dense, as bulldozers carrying out works will always work for longer periods.

For COO and ARGUS a set between 5 and 15 images were selected from each day with at least one visible bulldozer.

**2.4.1.3. Change image generation.** Performing change detection prior to the object detection has several advantages. In the first place it will improve the detection techniques as bulldozers moving will be highlighted in the images, while other elements that might lead to confusion (e.g. buildings, vegetation) will be deleted. Moreover, bulldozers that are static for long periods will not be detected as working bulldozers.

For the CoastScan dataset the images were grouped in sets of 15 images, which corresponds approximately to 34 min. For COO and ARGUS, images were grouped per day.

The  $n$  images of each group were transformed to grayscale and combined, generating a new image with  $n$  number of bands. PCA was computed for this newly generated image, resulting in  $n$  components.

The majority of the images information will be in the first components. Therefore, the first PCA component (PCA1) will correspond to the static elements, that are common between images. For each grayscale image a subtraction with PCA1 is computed, generating a change image (Fig. 5).

**2.4.1.4. Image cropping.** The images contain not only the sandy beach, but also other areas that have no interest for the study. The area of interest for each image was cropped. In order to get squared images that are recommended for YOLO's best performance, input images were decomposed into several adjacent, squared images for each of both camera viewpoints. For CoastScan camera 1, seven images of 320x320 pixels covering the beach area were obtained with an overlap of 20 pixels between consecutive ones. For CoastScan camera 2 only 3 images with same resolution and overlap were used, as the area further from the camera was discarded.

The COO and ARGUS images were also cropped to the same size and with the same overlap, following the same principle of maintaining only the beach area.

**2.4.1.5. Labelling.** The labelling process was carried out using the software Make Sense (Skalski, 2019). Bulldozers were identified in visible and change images separately.

**2.4.1.6. Model training.** The training was carried out for the original visible images and the change images separately.

All the images were labelled to identify the bulldozers, this was the only class taken into account.

The resulting RGB dataset was composed of 590 images (CoastScan: 408, COO: 113, Argus: 69). The change images dataset included 609



**Fig. 5.** Cropped visible original image (left) and corresponding change image highlighting the moving elements, a bulldozer and people standing on the beach (right).

images (CoastScan: 429, COO: 114, Argus: 66). The differences in numbers are due to different possibilities to identify the bulldozers. The datasets contained approximately 10 % of images without bulldozers as this amount of images is recommended for YOLO training.

Each dataset was split into train, validation and test (60 %, 20 %, 20 %).

The model was trained using the different models and pretrained weights available for YOLOv5, each training was computed once for each set of images (RGB and change). A maximum of 300 epochs was set.

In order to evaluate the improvement of the model by adding the COO and ARGUS images, a separate training was carried out using CoastScan images only.

**2.4.1.7. Model evaluation.** The best results were obtained with the pretrained model weights YOLOv5s. Therefore, the validation was carried out for this approach.

The models were evaluated using the test data, composed of 20 % of the images that were not used during model training or evaluation.

In order to have a detailed evaluation of the outcomes, the detection results for the test dataset were manually compared with the ground truth. The comparison was made element-wise. A detection was considered correct when the detected bulldozer visually fits a labelled bulldozer. Small differences in the edges of the object were not considered.

As the model was designed to be used on CoastScan Noordwijk data, a second evaluation of each approach was carried out on these data only.

#### 2.4.2. Automatic processing the whole CoastScan image dataset

Once the training stage was complete, the next step was to apply the methodology to process the whole CoastScan image dataset.

The process was carried out using a specifically designed tool for the images of Camera 1, as it covers the whole study area, and the derived information can be easily compared to the 3D data.

**2.4.2.1. Image extraction.** The CoastScan dataset is composed of folders containing a video or pre-extracted frames, along with a metadata file. The metadata file contains the specific acquisition time for each frame. Each folder contains the data for a time frame between 34 min and a day, depending on the image frequency.

In the first place, the created tool will read each metadata file and extract and copy the required frames to have a uniform time between consecutive images of 2.5 min. The name of each frame will correspond to the date and hour of acquisition.

Some images corresponded to night images. For each image, the mean of the RGB values was computed and, in case it was below a threshold of 110, it was considered too dark and removed.

**2.4.2.2. Image correction.** A camera calibration was carried out prior to the installation. For calibration, a chessboard pattern and Matlab Camera Calibrator App (Bouquet, 2004) was used to extract the calibration parameters, including: two components of the principal point, two components of focal length, three radial distortion coefficients, two tangential distortion coefficients and the skew. Knowing the calibration parameters, each frame was corrected using Python OpenCV (Bradski, 2000). The use of Python for image correction allowed to incorporate this stage in the automatic tool.

**2.4.2.3. Change detection and cropping.** After the images were extracted, the image change computation and cropping were carried out following the process described in Sections 2.4.1.3 and 2.4.1.4. The obtained dataset contained 18 719 input images and 112 314 cropped images.

**2.4.2.4. Bulldozer detection from images.** The detection was carried using the best performing previously trained YOLO model on the change images (see Section 3.1). For each image with a detected bulldozer a label file with the image coordinates and confidence of the detection were obtained.

**2.4.2.5. Image registration and coordinate extraction.** In order to use the obtained data to identify the anthropogenic changes we need to extract the coordinates of each detected bulldozer. In this way, the deformations can be located, and the information can be combined with the 3D data extracted from the laser scanner.

The external orientation parameters of the camera were extracted using ground reference points in the images.

As no stereography is available, it was not possible to extract the 3D coordinates of an image pixel from the images only. To solve this problem, a 3D point cloud taken by the CoastScan project scanner during low tide was used as a surface reference for the images.

A pseudo image of the scanner 3D data was created by reprojecting every point of the scan to an image with the same external orientation as the camera images. In this way, each pixel of the image was assigned a coordinate in the coordinate system of the scanner. A Z-buffering (Rossignac and Requicha, 1986) was used in case more than one 3D point corresponded to the same pixel, allowing to choose the point closest to the camera.

The accuracy of this methodology is affected by the changes in the sand surface and the height of the bulldozers. Nevertheless, we consider the obtained accuracy, in the order of a few meters, to be sufficient to give a location for the works carried out.

**2.4.2.6. Filtering.** The detected bulldozers are likely to present a high number of detections that do not correspond to machines carrying anthropogenic works in the sand. A filtering of the detections was therefore required to remove the following cases: (i) bulldozers passing by, only visible in one image, (ii) bulldozers outside the area of the sandy beach and (iii) static changes that are detected as bulldozers but correspond to other changes (e.g. turning on the lighting of the paths or buildings). Such static changes can be removed as the detection occurs in the same coordinates repeatedly.

To perform the filtering, the following detections were removed:

1. Isolated detections, when no more detections are carried out earlier or later for a time frame of two hours.
2. Detections out of the area of interest.
3. Consecutive detections with similar coordinates. A threshold of 3 pixels was established.

Two iterations of the process were carried out, so isolated detections are correctly identified after removing incorrect detections first.

## 2.5. Combination with other data sources

In order to understand and validate the obtained data, it is required to carry out a comparison with other data sources.

The results were compared with the daily maximum wind speed. The weekends were also considered as the works are expected to be reduced during these days.

The most important comparison was carried out with 3D data obtained by the permanent laser scanner.

### 2.5.1. Comparison with 3D data

Change analysis in 3D data is performed by computing distances between different scans. The process is detailed by [Kuschnerus et al. \(2021\)](#). The time difference between scans is one hour. An area is susceptible to anthropogenic change when there is a difference in height above 30 cm between two consecutive scans.

The number of changes susceptible of being anthropogenic, together with the affected area and volume were computed for each hour.

The correlation between the number of detected bulldozers and the area affected by possible anthropogenic changes in the 3D data was calculated. The correlation was calculated for both hourly and daily data.

A significant number of large changes in 3D data can have other causes but bulldozers, such as waves or parked cars. In order to isolate changes caused by bulldozers, a small area of the beach has been used for validation ([Fig. 6](#)). This area has dimensions of 27x47 m, is located close to the beach club building and is frequently affected by working bulldozers while other changes are limited as it is never covered by water and no cars or other disturbing elements are usually found. The changes in this area are assumed to be mostly caused by bulldozers.

## 3. Results

This section is structured in three parts, results regarding the training of the YOLO algorithm, results of the detection for the whole CoastScan dataset and comparison between the detected bulldozers and the changes derived from the 3D data.



**Fig. 6.** Validation area (in red). Image from Google Earth. (For interpretation of the references to colour in this figure legend, the reader is referred to the web version of this article.)

### 3.1. Evaluation of the detection algorithm

The element-wise evaluation of the YOLO detection is shown in Table 1. The evaluation was carried out for four training approaches: (i) using all change images (CoastScan, COO and ARGUS) (ii) using all original images (iii) using only CoastScan change images and (iv) using only CoastScan original images. Each evaluation was also performed both for all images and separately for CoastScan images only.

For each training and evaluation approach the number of true positives (TP), number of false positives (FP), accuracy (TP/(TP + FP)) and recall (TP/Instances) were calculated.

The best results were obtained for the model trained using all images and applied on the change images, resulting in a precision of 0.94 and a recall of 0.81. The detection process for all the images in the CoastScan dataset was performed using these model weights.

For every case, the model using change images performed better than the one using original RGB images. The training using all images provided better results than the training using CoastScan images only. In particular, using all images contributes to a lower number of false positives, and therefore, to a higher precision.

### 3.2. Bulldozer detection for the whole dataset

The bulldozer detection was computed for the whole dataset, consisting of 18 719 images. The results are shown in Fig. 7. The daily maximum wind speed is also displayed, and the weekends are highlighted. The graph shows a low number of detected bulldozers during the first weeks. A possible explanation for this low number is a limited maintenance activity in winter. This lower number of detections could also be partially caused by time gaps in the available video for the first 9 days. At the end of winter and the beginning of spring the number of detected working bulldozers increase drastically for a period of two weeks. After that, work seems to be kept at a lower level, probably for maintenance. In most cases, work is performed in days with low wind speed, right after storms or days with a much higher wind speed. The number of detections is lower on Saturdays and Sundays.

The visualization of the detections in the image is vital to understand the location of the changes and compare the 3D and image information. In Fig. 8 the detections for two days with different number of detections is visualized.

### 3.3. Comparison with changes derived from 3D data

Height changes above 30 cm between consecutive scans and detected bulldozers are presented in Fig. 9 for three different days. The location of detected changes and detected bulldozers are similar in the majority of cases.

The correlation between the area affected by height changes above 0.3 m and the number of detected bulldozers is presented in Table 1. For the whole area the correlation is low for a hourly time frame and significant when computed for a daily time frame. For the validation area, as it was to be expected, the correlation is higher, for the daily time frame the results show a strong positive correlation, with a value of 0.88 (Table 2).

**Table 1**

Element-wise classification evaluation results obtained on test data for CoastScan images and all images (CoastScan, COO and ARGUS), showing true positives (TP), false positives (FP), precision and recall, for change and original images. Best results in bold.

Images	Training	All images					CoastScan images only				
		Instances	TP	FP	Precision	Recall	Instances	TP	FP	Precision	Recall
Change	All images	120	93	8	0.92	0.78	83	67	4	<b>0.94</b>	<b>0.81</b>
Original	All images	121	90	14	0.87	0.74	78	61	9	0.87	0.78
Change	CoastScan						83	72	19	0.79	0.87
Original	CoastScan						78	51	11	0.82	0.65

## 4. Discussion

A method for automatic bulldozer detection on a large dataset has been presented. The detection process is hampered by the wide area covered by the images, leading to a small size of bulldozers in the images. Different meteorological conditions can also result in blurred images. This situation is common to many other image systems for coastal monitoring and would not allow the obtaining of good results using most common object detection techniques.

In this project, we propose a combination of PCA change detection and YOLO object detection. The algorithm was found to provide good results with a precision of 0.94 and recall of 0.81 for the CoastScan images. The change detection preprocessing improved the detection by slightly rising the recall and highly reducing the number of false positives in comparison to using YOLO directly on the original images. As the change detection is computed, most constant features or background of the images are removed, reducing the areas that can be misclassified as bulldozers. The change detection also allows for automatically removing static bulldozers, which may be parked on the beach for some periods but are not performing works in the sand.

The classification results are slightly better when images from other datasets (i.e. ARGUS and COO) are included in the training stage. These images added different locations and types of bulldozers, moreover, the lower frequency of the images led to noisier change images. This contributed to avoid overfitting during the training stage and significantly increased the final accuracy, with the caveat of a small loss in recall.

The coordinates of the detected bulldozers were also obtained. The accuracy in terms of georeferencing is considered to be in the order of 1–2 m and enough for location of works that include an area of several meters. The accuracy in the detection is also considered adequate. Small inaccuracies will very likely not affect the results, as a working bulldozer will likely be visible in many frames, decreasing the importance of a false negative. In the same way, another vehicle that is not working on the sand is not likely to be moving around during a long time period, and therefore, it can be easily removed as a possible working bulldozer.

With a frame frequency of one image each 2.5 min the implemented methodology can easily be run in real time. Therefore, it is suitable for processing the large quantities of data generated by continuous monitoring systems.

The bulldozer detection results were compared with the changes derived from the 3D models. The distribution of changes and bulldozers for particular days is presented and can be used for classification of the changes. The correlation between changes and number of detected bulldozers is strong for a validation area and a daily time frame, while hourly comparison has a lower correlation. Several reasons can explain low correlation values. In the first place, 3D data derived changes can have different causes and it is difficult to isolate anthropogenic changes by using only a threshold in height differences. The higher correlation for a limited study area reinforces this point. The important differences in correlation when hourly time frames are used points to a time difference between the detection of the bulldozers and the detection of the changes. In some cases, bulldozers are probably detected when on their way to the work area, on their way back or when they are parked during shift changes or breaks. As a consequence, we can conclude that the



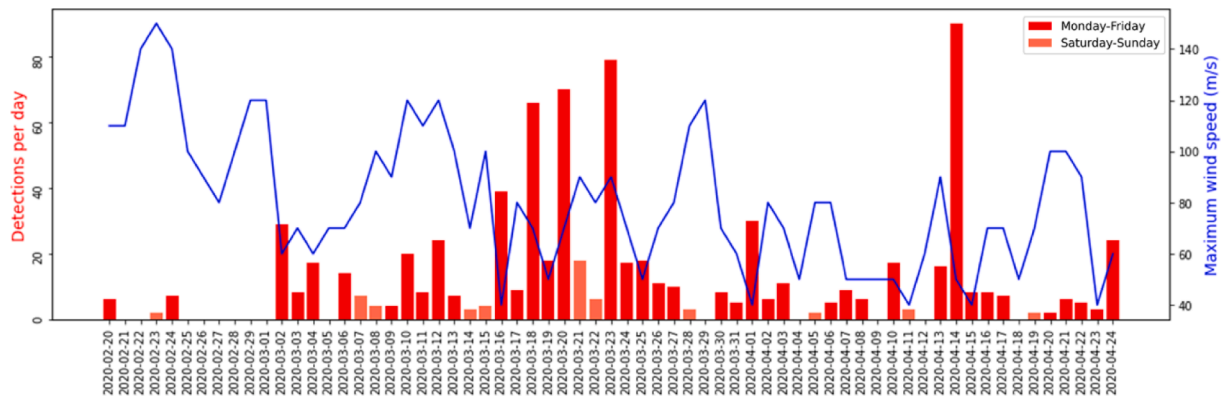


Fig. 7. Detected bulldozers (red) for the full period and maximum wind speed (blue). Weekends are indicated by orange bars. (For interpretation of the references to colour in this figure legend, the reader is referred to the web version of this article.)

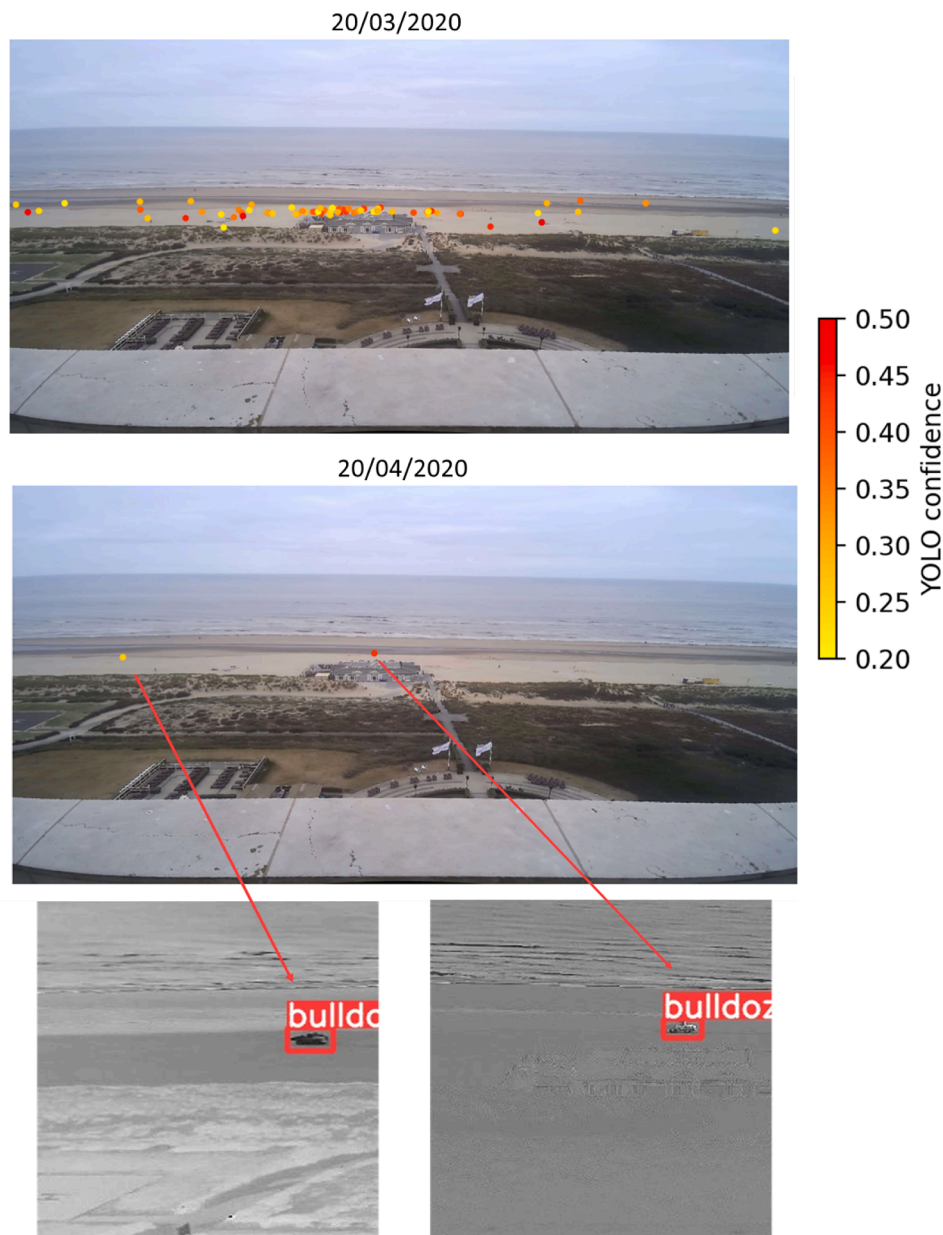


Fig. 8. Detections of bulldozers for two given days and colors according to YOLO confidence and change images with detected bulldozers for the second date.

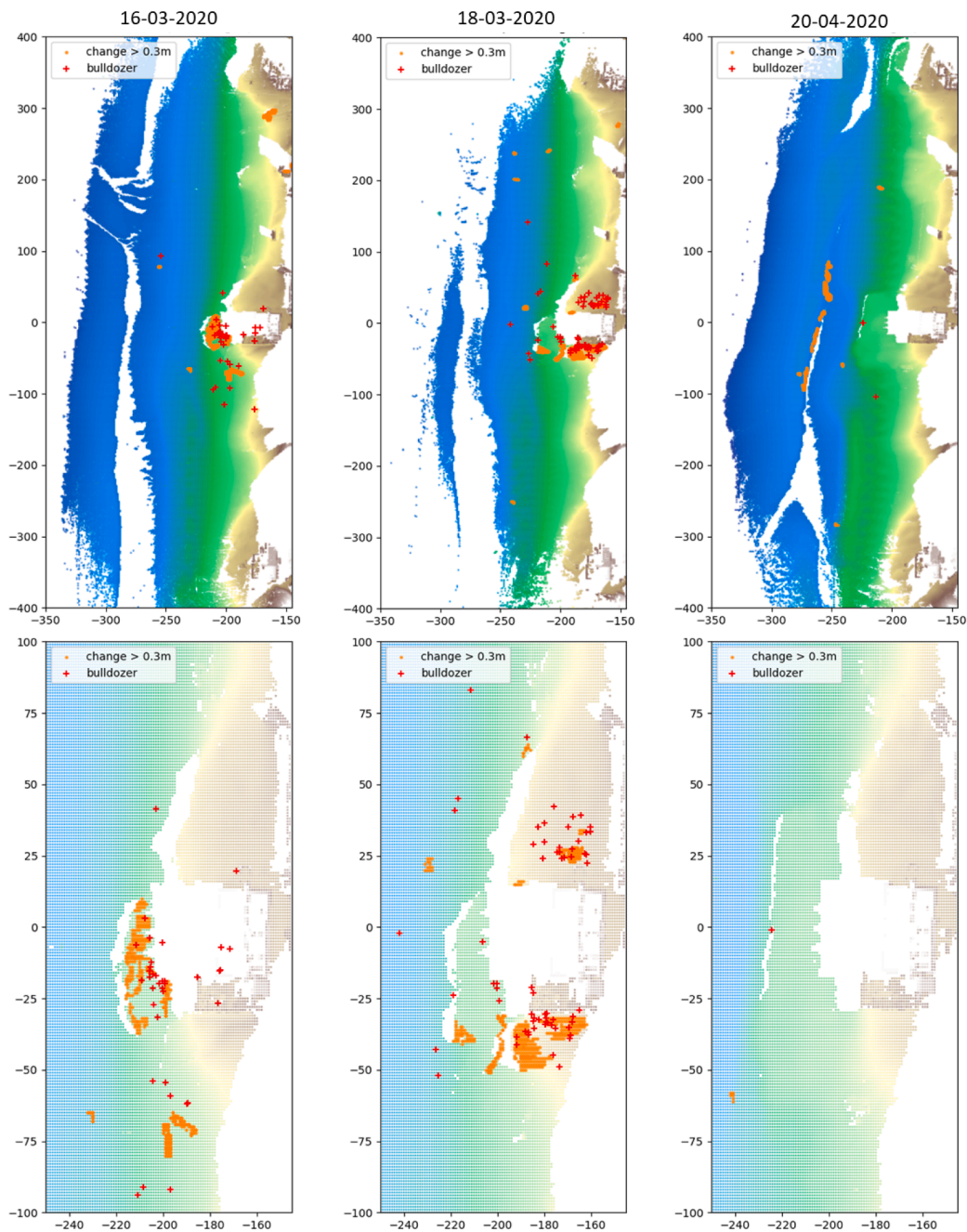


Fig. 9. Maps of scan-derived changes larger than 30 cm and detected bulldozers for different days for the whole area (top), and for the area closer to the beach club building (bottom).

Table 2

Correlation results between the number of detected bulldozers and the area affected by changes above 30 cm according to the 3D data.

Time frame	Area of study	Correlation
Hourly	Whole study area	0.29
Daily	Whole study area	0.57
Hourly	Validation area	0.43
Daily	Validation area	0.88

determination of the working time of the bulldozers can only be obtained with a margin of several hours. Lastly, bulldozers can be doing work that does not create an important change in surface height, such as flattening a slightly wavy area or even carrying objects.

The results show that the number of detected bulldozers is correlated

to the area affected by anthropogenic changes. The information obtained using object detection can be used to support and validate the classification of anthropogenic and natural changes measured using other techniques.

The technique has the objective of identifying bulldozers, understood as heavy motorized machines capable of carrying a blade or digging and therefore, suited to move large quantities of sand. The variability of these machines in size, shape and other characteristics is wide. They can also be mistaken to pickups or other vehicles commonly driven around the beach by conservation or vigilance services. In the presented study, training data from three different locations was employed. Despite of this, the variability of the area and the vehicles identified is still limited. In order to apply the presented technique to other locations, it would be necessary to assure that the model adapts to the characteristics of the new location and the machines employed. In

some cases, a new training might be required. Apart from this necessity, the methodology could easily be employed in other coastal monitoring projects for locations with similar characteristics (similar visibility conditions).

Future works will include a larger correlation with 3D data deformations. A threshold of the number of detected bulldozers in a location and time frame to classify changes as anthropogenic should be derived. Other object detection algorithms could also be tested.

## 5. Conclusion

In this study we have presented a methodology to automatically detect working bulldozers from coastal imagery. The images used are generated by a camera placed near to the coast as part of the CoastScan project.

Machine learning object detection, in particular the combination of YOLO and PCA change detection, have proven to be capable to automatically detect and quantify human interventions in beaches. The presented methodology can contribute to the better understanding of coastal processes by differencing anthropogenic and natural changes. It could be implemented on different spots, especially those hotspots more susceptible to erosion and human activity, in order to obtain important information for conservation and management. It can be applied to low-cost data and already available data, such as imagery extracted from surfcams (cameras installed on the coast with the objective to provide surfers and beachgoers with real time information on the sea state by streaming video on the internet) (Andriolo et al., 2019) or other coastal monitoring systems. It can also complement other types of data like 3D data extracted from laser scanner.

As the anthropogenic changes caused by bulldozers potentially have a great impact on beach ecosystems, a detailed detection and monitoring of these changes is helpful to improve coastal management. In particular, it can help enforce and improve regulations, thereby contributing to limit the impact to economy and fauna of coastline retreat, while helping in objectives as presented in the Sustainable Development Goals.

## CRedit authorship contribution statement

**Inés Barbero-García:** Methodology, Software, Validation, Formal analysis, Visualization, Writing – original draft. **Mieke Kuschnerus:** Validation, Formal analysis, Visualization, Writing – review & editing. **Sander Vos:** Data curation, Funding acquisition. **Roderik Lindenbergh:** Conceptualization, Methodology, Writing – review & editing, Supervision, Project administration, Funding acquisition.

## Declaration of Competing Interest

The authors declare that they have no known competing financial interests or personal relationships that could have appeared to influence the work reported in this paper.

## Data availability

The data presented in the paper can be accessed via repository: [https://github.com/IBarberoGarcia/YOLO\\_bulldozer\\_detection](https://github.com/IBarberoGarcia/YOLO_bulldozer_detection). Contact: ines.barbero@usal.es.

## Acknowledgements

This research has been supported by the Netherlands Organization for Scientific Research (NWO, grant no. 16352) as part of the Open Technology Programme and by Rijkswaterstaat (Dutch Ministry of Infrastructure and Water Management).

## References

- Abdi, H., Williams, L.J., 2010. Principal component analysis. *WIREs Comput. Stat.* 2 (4), 433–459. <https://doi.org/10.1002/wics.101>.
- Anders, K., Winiwarter, L., Mara, H., Lindenbergh, R., Vos, S.E., Bernhard, H., 2021. Fully automatic spatiotemporal segmentation of 3D LiDAR time series for the extraction of natural surface changes. *ISPRS J. Photogramm. Remote Sens.* 173, 297–308. <https://doi.org/10.1016/j.isprsjprs.2021.01.015>.
- Andriolo, U., Sánchez-García, E., Taborda, R., 2019. Operational use of surfcam online streaming images for coastal morphodynamic studies. *Remote Sensing* 11(1), 78. doi: 10.3390/RS11010078.
- Barros, F., 2001. Ghost crabs as a tool for rapid assessment of human impacts on exposed sandy beaches. *Biol. Conserv.* 97 (3), 399–404. [https://doi.org/10.1016/S0006-3207\(00\)00116-6](https://doi.org/10.1016/S0006-3207(00)00116-6).
- Bouguet, J.-Y., 2004. Camera calibration toolbox for matlab. [http://www.vision.caltech.edu/bouguet/calib\\_doc/index.html](http://www.vision.caltech.edu/bouguet/calib_doc/index.html).
- Bradski, G., 2000. The OpenCV Library. Dr. Dobb's J. Software Tools.
- Conlin, M.P., Adams, P.N., Wilkinson, B., Dusek, G., Palmsten, M.L., Brown, J.A., 2020. SurfRCaT: A tool for remote calibration of pre-existing coastal cameras to enable their use as quantitative coastal monitoring tools. *SoftwareX* 12, 100584. <https://doi.org/10.1016/J.SOFTX.2020.100584>.
- Costa, L.L., Fanini, L., Zalmon, I.R., Defeo, O., McLachlan, A., 2022. Cumulative stressors impact macrofauna differentially according to sandy beach type: a meta-analysis. *J. Environ. Manage.* 307, 114594.
- Davenport, J., Davenport, J.L., 2006. The impact of tourism and personal leisure transport on coastal environments: a review. *Estuar. Coast. Shelf Sci.* 67 (1–2), 280–292. <https://doi.org/10.1016/j.ecss.2005.11.026>.
- de Andrade, T.S., Sousa, P.H.G. de O., Siegle, E., 2019. Vulnerability to beach erosion based on a coastal processes approach. *Appl. Geogr.* 102, 12–19. doi: 10.1016/j.apgeog.2018.11.003.
- de Schipper, M.A., Ludka, B.C., Raubenheimer, B., Luijendijk, A.P., Schlacher, T., 2021. Beach nourishment has complex implications for the future of sandy shores. *Nat. Rev. Earth Environ.* 2 (1), 70–84.
- Defeo, O., McLachlan, A., Schoeman, D.S., Schlacher, T.A., Dugan, J., Jones, A., Lastra, M., Scapini, F., 2009. Threats to sandy beach ecosystems: a review. *Estuar. Coast. Shelf Sci.* 81 (1), 1–12. <https://doi.org/10.1016/J.ECSS.2008.09.022>.
- Deng, J.S., Wang, K., Deng, Y.H., Qi, G.J., 2008. PCA-based land-use change detection and analysis using multitemporal and multisensor satellite data. *Int. J. Remote Sens.* 29 (16), 4823–4838. <https://doi.org/10.1080/01431160801950162>.
- Holman, R.A., Stanley, J., 2007. The history and technical capabilities of Argus. *Coast. Eng.* 54 (6–7), 477–491. <https://doi.org/10.1016/J.COASTALENG.2007.01.003>.
- Ingebritsen, S.E., Lyon, R.J.P., 1985. Principal components analysis of multitemporal image pairs. *Int. J. Remote Sens.* 6 (5), 687–696. <https://doi.org/10.1080/01431168508948491>.
- Jalal, A., Salman, A., Mian, A., Shortis, M., Shafait, F., 2020. Fish detection and species classification in underwater environments using deep learning with temporal information. *Ecol. Inform.* 57, 101088 <https://doi.org/10.1016/J.ECOINF.2020.101088>.
- Kandrot, S., Hayes, S., Holloway, P., 2022. Applications of uncrewed aerial vehicles (UAV) technology to support integrated coastal zone management and the UN sustainable development goals at the coast. *Estuar. Coasts* 45 (5), 1230–1249. <https://doi.org/10.1007/s12237-021-01001-5>.
- Kuschnerus, M., Lindenbergh, R., Lodder, Q., Brand, E., Vos, S., 2022. Detecting anthropogenic volume changes in cross sections of a sandy beach with permanent laser scanning. In: *The International Archives of the Photogrammetry, Remote Sensing and Spatial Information Sciences, XLIII-B2-2022*, 1055–1061. doi: 10.5194/isprs-archives-XLIII-B2-2022-1055-2022.
- Kuschnerus, M., Lindenbergh, R., Vos, S., 2021. Coastal change patterns from time series clustering of permanent laser scan data. *Earth Surf. Dyn.* 89–103 <https://doi.org/10.5194/esurf-9-89-2021>.
- Kuschnerus, M. et al., 2022. Detecting anthropogenic volume changes in cross sections of a sandy beach with permanent laser scanning. In: *The International Archives of the Photogrammetry, Remote Sensing and Spatial Information Sciences. XXIV ISPRS Congress "Imaging today, foreseeing tomorrow"*, Commission II - 2022 edition, 6–11 June 2022, Nice, France, Copernicus GmbH, pp. 1055–1061. doi: 10.5194/isprs-archives-XLIII-B2-2022-1055-2022.
- Landry, C.E., 2011. Coastal Erosion as a natural resource management problem: an economic perspective. *Coast. Manag.* 39 (3), 259–281. <https://doi.org/10.1080/08920753.2011.566121>.
- Lazarus, E.D., Goldstein, E.B., 2019. Is there a bulldozer in your model? *J. Geophys. Res.* Earth 124 (3), 696–699. <https://doi.org/10.1029/2018JF004957>.
- Lin, F., Hou, T., Jin, Q., You, A., 2021. Improved YOLO based detection algorithm for floating debris in waterway. *Entropy* 23 (9), 1111. <https://doi.org/10.3390/E23091111>.
- Lazarus, E.D., McNamara, D.E., Smith, M.D., Gopalakrishnan, S., Murray, A.B., 2011. Emergent behavior in a coupled economic and coastline model for beach nourishment. *Nonlinear Processes Geophys.* 18 (6), 989–999. <https://doi.org/10.5194/npg-18-989-2011>.
- List, J.H., Farris, A.S., Sullivan, C., 2006. Reversing storm hotspots on sandy beaches: spatial and temporal characteristics. *Mar. Geol.* 226 (3), 261–279. <https://doi.org/10.1016/j.margeo.2005.10.003>.
- Lu, D., Mausel, P., Batistella, M., Moran, E., 2005. Land-cover binary change detection methods for use in the moist tropical region of the Amazon: a comparative study. *Int. J. Remote Sens.* 26 (1), 101–114. <https://doi.org/10.1080/01431160410001720748>.

- Luijendijk, A., Hagenaars, G., Ranasinghe, R., Baart, F., Donchyts, G., Aarninkhof, S., 2018. The state of the world's beaches. *Sci. Rep.* 8 (1), 1. <https://doi.org/10.1038/s41598-018-24630-6>.
- Magliocca, N.R., McNamara, D.E., Murray, A.B., 2011. Long-term, large-scale morphodynamic effects of artificial dune construction along a Barrier Island Coastline. *J. Coast. Res.* 27 (5), 918–930. <https://doi.org/10.2112/JCOASTRES-D-10-00088.1>.
- Masoom, S.M., Zhang, Q., Dai, P., Jia, Y., Zhang, Y., Zhu, J., Wang, J., 2022. Early smoke detection based on improved YOLO-PCA network. *Fire* 5 (2), 2. <https://doi.org/10.3390/fire5020040>.
- Mentaschi, L., Voudoukas, M.I., Pekel, J.-F., Voukouvalas, E., Feyen, L., 2018. Global long-term observations of coastal erosion and accretion. *Sci. Rep.* 8 (1), Art. 1. <https://doi.org/10.1038/s41598-018-30904-w>.
- Nieto, M.A., Garau, B., Balle, S., Simarro, G., Zarruk, G.A., Ortiz, A., Tintoré, J., Álvarez, A., Gómez, L., Orfila, A., 2010. An open source, low cost video-based coastal monitoring system. *Earth Surf. Processes Landforms* 35 (14), 1712–1719. <https://doi.org/10.1002/ESP.2025>.
- Paprotny, D., Terefenko, P., Giza, A., Czaplinski, P., Voudoukas, M.I., 2021. Future losses of ecosystem services due to coastal erosion in Europe. *Sci. Total Environ.* 760, 144310 <https://doi.org/10.1016/j.scitotenv.2020.144310>.
- Peterson, C.H., Bishop, M.J., 2005. Assessing the environmental impacts of beach nourishment. *Bioscience* 55 (10), 887–896. [https://doi.org/10.1641/0006-3568\(2005\)055\[0887:ATEIOB\]2.0.CO;2](https://doi.org/10.1641/0006-3568(2005)055[0887:ATEIOB]2.0.CO;2).
- Puliti, S., Astrup, R., 2022. Automatic detection of snow breakage at single tree level using YOLOv5 applied to UAV imagery. *Int. J. Appl. Earth Obs. Geoinf.* 112, 102946 <https://doi.org/10.1016/j.jag.2022.102946>.
- Quartel, S., Addink, E.A., Ruessink, B.G., 2006. Object-oriented extraction of beach morphology from video images. *Int. J. Appl. Earth Observ. Geoinform.* 8 (4), 256–269.
- Redmon, J., Divvala, S., Girshick, R., & Farhadi, A. (2016). You only look once: Unified, real-time object detection. In: *Proceedings of the IEEE Computer Society Conference on Computer Vision and Pattern Recognition*, 2016-December, pp. 779–788. doi: 10.1109/CVPR.2016.91.
- Rossignac, J.R., Requicha, A.A.G., 1986. Depth-buffering display techniques for constructive solid geometry. *IEEE Comput. Graph. Appl.* 6 (9), 29–39. <https://doi.org/10.1109/MCG.1986.276544>.
- Ruessink, B.G., Jeuken, M.C.J.L., 2002. Dunefoot dynamics along the Dutch coast. *Earth Surf. Processes Landforms: J. Br. Geomorphol. Res. Group* 27 (10), 1043–1056.
- Skalski, P., 2019. Make Sense. Available at: <https://github.com/SkalskiP/make-sense/>.
- Stronkhorst, J., Huisman, B., Giardino, A., Santinelli, G., Santos, F.D., 2018. Sand nourishment strategies to mitigate coastal erosion and sea level rise at the coasts of Holland (The Netherlands) and Aveiro (Portugal) in the 21st century. *Ocean Coast. Manag.* 156, 266–276. <https://doi.org/10.1016/j.ocecoaman.2017.11.0>.
- Taborda, R., Silva, A., 2012. COSMOS: a lightweight coastal video monitoring system. *Comput. Geosci.* 49, 248–255. <https://doi.org/10.1016/J.CAGEO.2012.07.013>.
- United Nations, 2015. COP21 (United Nations Framework Convention on Climate Change). Paris. [https://unfccc.int/sites/default/files/english\\_paris\\_agreement.pdf](https://unfccc.int/sites/default/files/english_paris_agreement.pdf).
- Veerasingam, S., Chatting, M., Asim, F.S., Al-Khayat, J., Vethamony, P., 2022. Detection and assessment of marine litter in an uninhabited island, Arabian Gulf: a case study with conventional and machine learning approaches. *Sci. Total Environ.* 838, 156064 <https://doi.org/10.1016/j.scitotenv.2022.156064>.
- Vos, S., Lindenbergh, R.C., De Vries, S., Lindenbergh, R., 2017. Coastscan: Continuous monitoring of coastal change using terrestrial laser scanning Change Detection View project The Influence of Intertidal Sandbar Welding on Dune Growth View project COASTSCAN: CONTINUOUS MONITORING OF COASTAL CHANGE USING TERRESTRIAL. *Coast. Dyn.* 2017, 1518–1528.
- Vos, S., Anders, K., Kuschnerus, M., Lindenbergh, R., Höfle, B., Aarninkhof, S., de Vries, S., 2022. A high-resolution 4D terrestrial laser scan dataset of the Kijkduin beach-dune system. *The Netherlands Sci. Data* 9 (1), Art. 1. <https://doi.org/10.1038/s41597-022-01291-9>.
- Xu, R., Lin, H., Lu, K., Cao, L., Liu, Y., 2021. A forest fire detection system based on ensemble learning. *Forests* 12(2), 217. doi: 10.3390/F12020217.